On a method for parametric representation of the state of the atmosphere

By INGEMAR HOLMSTRÖM, *International Meteorological Institute, Stockholm*[1]

(Manuscript received February 5, 1963)

ABSTRACT

In a discussion of possible parametric representations of the state of the atmosphere it is shown that the common use in numerical prediction models of parameters directly given by the height of certain pressure levels is inefficient. An alternative method is suggested where atmospheric variables are expanded in empirical orthogonal functions. The expansion takes for height data the form

$$Z(x, y, t, p) = F_0(p) + \sum_{1}^{K} z_k(x, y, t)\, F_k(p),$$

where $F_0(p)$ represents an area average and the functions $F_k(p)$ and the coefficients $z_k(x, y, t)$ are determined using a least square residual condition and a condition of finality.

Expansions of this type have been made on height and wind data for eight days. Results from these expansions are given. The convergence is found to be surprisingly rapid and two or at most three modes are sufficient for an accurate description of the large scale structure of the troposphere and the lower stratosphere. The form of the pressure functions in the lowest modes is found to be approximately conservative.

Finally, maps of the coefficient fields are presented and a brief discussion given of a case of pronounced baroclinic development.

1. Introduction

The experience from numerical forecasting during the past decade has very clearly shown that the equivalent barotropic model represents a surprisingly good first approximation to the atmosphere. During the same period it has also become evident that baroclinic models, even though they seem to provide for a more correct and detailed description of the vertical structure of the atmosphere, do not increase forecasting accuracy in the middle troposphere. The reason for this is not yet known. Except in a few respects, recently reviewed by GATES (1961*a*), we have no means to decompose the complex error fields of a forecast into components directly related to different kinds of model approximations. The research aiming at improved forecasting will therefore to a large extent have to be based on a method of trial and error and on informed guesses.

Here a further difficulty is that a test will be conclusive only if a definite improvement is obtained. A negative result, like the persistent failure of baroclinic models to meet expectations of better forecasts, may indicate that in a second approximation to the atmosphere one should also include some or several other factors, friction, topography, nonadiabatic heating, small order terms in the equations, etc. But it is equally possible that the poor results are due to an inefficient choice of the parameters in the model which should represent the baroclinic state of the atmosphere.

In order to investigate this point in an ideal case one would have to determine some *necessary* conditions that a set of forecasting parameters should fulfill with regard not only to their determination from available initial data and to their use for representation of some wanted fields in a forecast atmosphere, but also and in particular to the requirement that they should

[1] The research reported in this article has been sponsored in part by the Cambridge Research Laboratories, OAR, through the European Office, Aerospace Research U.S. Air Force.

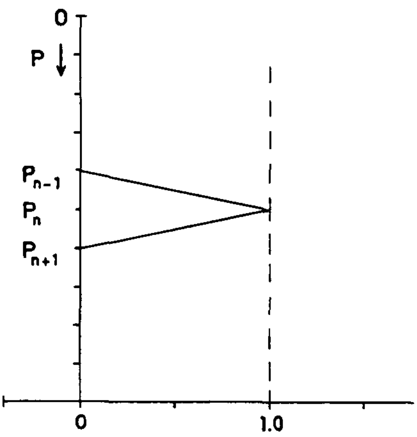

FIG. 1. Influence function in finite difference model.

be suitable and efficient when introduced in the forecasting equations. Even if this latter condition has been considered to varying degrees in existing models, it is not easily formulated in a precise way. One may, however, avoid this difficulty by using instead a more general condition of maximum descriptive capacity of the parameters, a condition which is probably not necessary but certainly will be sufficient since it implies that at each instant and with given values of the parameters one should be able to describe correctly the state of the atmosphere at all heights and thus also have basic data for computation of local time derivatives.

With this change in the intentions the problem has been brought to a point where sufficient information can be obtained from a statistical treatment of observational data. It has also in a certain sense become more general with obvious implications in the field of data handling and transmission and in general for descriptive and statistical purposes.

It is natural with regard to the observations that we should limit ourselves to the pressure interval 1000–100 mb and also that in the first instant we consider the use of height data. It is the intention in the following section to discuss a few possible methods for this representation and to investigate more closely the one that seems to give the best result with regard to the number of parameters required for a certain accuracy.

2. Series expansions

In an ordinary finite difference model the height field may be expressed through a series expansion of the form

$$Z(p,x,y) = a_1(p)\,Z_1(p_1,x,y) + \dots + a_n(p)\,Z_n(p_n,x,y) \tag{2.1}$$

where $p_1,\dots,p_n$ are the levels for which the heights $Z_1,\dots,Z_n$ are given and the functions $a_1(p),\dots,a_n(p)$ are stepwise linear influence functions of the form given in Fig. 1. This expansion, which admits computation of first order vertical derivatives, will have large residuals at intermediate levels if the number of terms is kept within reasonable limits. A first improvement may be obtained by using the observed fact that the atmosphere has a well defined average vertical structure around which the variations are relatively small. We therefore define a horizontally averaged height function $F_0(p)$ by

$$F_0(p) = \frac{1}{S}\int_S Z(p,x,y)\,dS, \tag{2.2}$$

where S is a large area, comparable with the size of a hemisphere. We further define deviations $z(p,x,y)$ from this standard atmosphere through

$$z(p,x,y) = Z(p,x,y) - F_0(p). \tag{2.3}$$

The time dependence has been left out of consideration, since for the moment we are interested only in conditions at one given time. It is to be expected, however, that time variations in $F_0(p)$ will in general be small and mostly of a seasonal character if S is chosen sufficiently large. Evidence for this will be given later when numerical results are discussed.

A second improvement may be obtained if we further observe that there exists in the atmosphere a vertical coupling between the deviations at different levels which is sufficiently strong to keep characteristic scales and phase-speeds almost independent of height. By giving the influence functions a more general form one can use the interrelation between the levels $p_1,\dots,p_n$ to exclude some of the terms in the series expansion and still have the desired accuracy. In order to determine the levels that should be retained because they provide the most efficient parameters, we write the expansion of the height deviations formally as

$$z(p, x, y) = \sum_{k=1}^{n} a_k(p)\, z_k(p_k, x, y) - r(p, x, y) \tag{2.4}$$

and require, using the ordinary least squares method, that the variance of the residual $r(p,x,y)$ should be minimum when integrated over the total mass of the atmosphere. The total variance is

$$R = \frac{1}{SP} \int_S \int_P \left[z - \sum_1^n a_k z_k \right]^2 dS dp, \tag{2.5}$$

where P represents the pressure interval, 100–1000 mb.

Taking the variation of (2.5) with respect to $p_1, ..., p_n$, we obtain the conditions for a stationary value of R

$$\left.\begin{aligned} &\int_S \int_P [z - \textstyle\sum a_k z_k]\, a_1 \left(\frac{\partial z}{\partial p}\right)_{p=p_1} dS dp = 0, \\ &\int_S \int_P [z - \textstyle\sum a_k z_k]\, a_2 \left(\frac{\partial z}{\partial p}\right)_{p=p_2} dS dp = 0, \\ &\quad \vdots \\ &\text{etc.} \end{aligned}\right\} \tag{2.6}$$

This system is made complete through a variation with respect to $a_1(p), ..., a_n(p_n)$, where we have to observe that the variation in these functions should be arbitrary for each value of p. The pressure integrals are therefore eliminated and the result is

$$\left.\begin{aligned} &\int_S [z - \textstyle\sum a_k z_k]\, z_1 dS = 0, \\ &\int_S [z - \textstyle\sum a_k z_k]\, z_2 dS = 0, \\ &\quad \vdots \\ &\text{etc.} \end{aligned}\right\} \tag{2.7}$$

Since the unknown pressure levels $p_1, ..., p_n$ do not enter explicitly in the system (2.6) and (2.7) we cannot in a direct way obtain the solutions from given data on z. The procedure to follow in numerical machine computations will not be discussed here in any detail since the system will be the subject of a special investigation to be reported later. For our present purpose it is sufficient to point out that one may determine two different types of solutions.

In the first case one has to decide beforehand the number, n, of parameters to be used. The system (2.6) and (2.7) is then solved by testing the total residual R in a systematic way for different combinations of $p_1, ..., p_n$; the functions $a_1(p), ..., a_n(p)$ being determined from (2.7) for each combination. The procedure is not very complicated if n is small but it is possible that several combinations may be equally good. With this method the expansion (2.4) will not have the character of a convergent series since the terms will be of equal importance. The result is that the pressure levels and the functions will not have a property of finality since addition of one more parameter will necessitate a recomputation.

In the second case the condition of minimum residual is successively applied for each additional term in (2.4). With this requirement of finality maximum convergence is ensured for each step in the expansion and the first term will be dominant. This means that $a_1(p)$ will reflect a mean structure of the height deviations and, due to quasigeostrophic balance, be similar to the function $A(p)$ for the variation of wind with height, first introduced by CHARNEY (1949) in connection with the definition of the equivalent barotropic atmosphere. The following terms in the expansion will then show the deviations from this general state.

The advantage obtained through this possibility of interpreting the results and the further advantage of having in a prognostic system parameters that are of different orders of magnitude and therefore will allow for rational approximations, has here been taken as a sufficient reason for adopting the requirement of finality as a principle in the expansion.

We have so far only considered parameters that are directly given through the heights of certain pressure levels. This has in fact restricted our possibilities of obtaining a fast convergence. In order to show this, consider the relation obtained from (2.7) for determining $a_1(p)$. It is

$$\int_S z z_1 dS = a_1(p) \int_S z_1^2 dS.$$

Let us now multiply (2.4) by $z_1(p_1, x, y)$ and integrate over S. Taking the relation above into account, we find

$$0 = a_2(p) \int_S z_1 z_2 dS + a_3(p) \int_S z_1 z_3 dS + \cdots$$

It is seen, that if $a_2(p), ..., a_n(p)$ were independent functions, then each area integral should vanish separately. Due to the vertical coupling it is clearly not possible to find an arbitrary number of height fields that are uncorrelated with $z_1(p_1,x,y)$. The pressure functions $a_1(p), ..., a_n(p)$ are therefore necessarily correlated in the vertical and contain to some extent common information. The disadvantage of not utilizing the full descriptive capacity of the parameters seems to have been first pointed out by BOLIN (1953) in a general discussion of multiparameter models. It may be avoided here, however, if in (2.4) we drop the requirement of directly given values for the parameters. Let us restate the expansion as

$$z(p,x,y) = \sum_1^n z_k(x,y)\, F_k(p) + r(p,x,y), \tag{2.8}$$

where the coefficients now are undetermined functions of x and y and the notation for the pressure functions has been changed. Since numerical values are not fixed for z_k or F_k, we need here a normalizing condition. The most convenient is

$$\frac{1}{P}\int_P F_k^2\, dp = 1, \tag{2.9}$$

since it will give values to the co-efficients z_k that are comparable with the height variations of a pressure surface. We now apply the same minimum condition to the residual as before and also a condition of finality. This gives the following set of equations

$$\left.\begin{aligned}
&\frac{1}{P}\int_P zF_1\, dp = z_1, \qquad \int_S zz_1\, dS = F_1 \int_S z_1^2 dS;\\
&\frac{1}{P}\int_P (z - z_1F_1)\, F_2\, dp = z_2, \qquad \int_S (z - z_1F_1)\, z_2\, dS\\
&\qquad\qquad = F_2 \int_S z_2^2 dS;\\
&\quad\vdots\\
&\frac{1}{P}\int_P \left(z - \sum_1^{n-1} z_k F_k\right) F_n\, dp = z_n,\\
&\qquad \int_S \left(z - \sum_1^{n-1} z_k F_k\right) z_n\, dS = F_n \int_S z_n^2\, dS,
\end{aligned}\right\} \tag{2.10}$$

where use has been made of (2.9). The first pair of equations forms a complete set for determination of $z_1(x,y)$ at all the points and of $F_1(p)$ for all the pressure levels for which $z(p,x,y)$ is given. With this solution known, the second pair of equations can be solved and so on.

In order to prove the expected orthogonality properties of the expansion we multiply the first equation in the first pair by z_2 and integrate over S and the second equation in the second pair by F_1 and take a vertical average. We find

$$\frac{1}{P}\int_P \int_S zz_2 F_1\, dp dS = \int_S z_1 z_2\, dS,$$

$$\frac{1}{P}\int_P \int_S zz_2 F_1\, dp dS - \int_S z_1 z_2\, dS = \frac{1}{P}\int_P F_1 F_2\, dp \int_S z_2^2 dS.$$

It is obvious from these two equations that F_1 and F_2 must be orthogonal since the integrated value of z_2^2 cannot vanish. By using the remaining two equations it is easily shown that also z_1 and z_2 are orthogonal over S. Extending the proof we have

$$\left.\begin{aligned}
&\frac{1}{P}\int_P F_k F_m\, dp = \begin{cases} 1 & \text{if} \quad k = m,\\ 0 & \text{if} \quad k \neq m,\end{cases}\\
&\int_S z_k z_m\, dS = 0 \qquad \text{if} \quad k \neq m,
\end{aligned}\right\} \tag{2.11}$$

These properties ensure that the expansion in what may be called *empirical orthogonal functions* will give the fastest possible convergence and that, with certain limitations due to the condition of finality, a minimum number of parameters will be required for a description of a given accuracy. The expansion has here been discussed in terms of height values but is naturally quite general and may be used for analysis of any set of data where some kind of regular behaviour is expected along the axis of one of the independent variables.

Since the method is not well known and its application to meteorological problems seems promising,[1] it is the intention here to give a

[1] Reference should here be made to a paper by OBUKHOV (1960), published during an early stage of this work, where an identical form of expansion was derived. Obukhov applied it to two cases of

rather detailed account of some of the results that during the course of a more general investigation have been obtained by expanding height, wind and to some extent also temperature data. This will also provide a suitable background for a following paper where an attempt is made to apply the results to the thermohydrodynamic system of equations.

3. Computational procedure and basic data

In the program for solving the system (2.10), together with the condition (2.9) and the relations (2.2) and (2.3), all horizontal integrations have been replaced by a pure summation over available data, independent of the network density. This means that continental areas have been highly overrepresented, while areas with poor data coverage have been given little weight. The reason has been a desire to simplify the computations and the preparation of data and also to avoid the very large influence that observational errors in soundings from remote stations otherwise would have.

Integrations over the pressure interval 1000–100 mb were made using the trapezoidal rule in steps varying between 50 and 200 mb. After determination of F_0 and z (eq. (2.2) and (2.3)) the first pair of equations in (2.10) was solved by an iterative procedure, using a first guess on F_1. The convergence was rapid even with a crude first guess. With known values for z_1 and F_1 for all stations and all levels, the residuals $z - z_1 F_1$ were computed and the second pair of equations in (2.10) solved for z_2 and F_2 through the same iterative procedure, using a first guess on F_2, etc.

The first computations of this type were carried out using the Swedish computer BESK on 256 temperature and wind soundings from 00 GMT, June 18, 1959. In order to simplify the preparation of data the levels 1000, 850, 700, 500, 400, 300, 200, 150 and 100 mb were chosen. Soundings not reaching 100 mb were discarded. Missing height values for the intermediate pressure levels were obtained through interpolation on a z-log$p$ diagram and missing height values for the 1000 mb level through extrapolation from the nearest higher level on the assumption of a temperature gradient of 0.55°/100 m. Only 5–10 per cent of the soundings needed completion in this way.

The wind data were divided into u and v components and when necessary interpolated, assuming a linear variation with height. The same levels as for the heights were used, including 1000 mb, where for simplicity the wind was assumed to vanish. The wind components were expanded separately and without first taking a horizontal average. The computations for this day were continued up to the fourth mode and the program also included determination of r.m.s. values of the coefficients and the residuals.

The analysis of the results from 18.6.1959 and from a few preliminary tests showed the need for a more comprehensive and detailed study. For this purpose data were prepared for a period, 21.10.1959–27.10.1959 (which is hereafter referred to as "the October period") during which pronounced baroclinic developments took place. A new and more complete program was made for use on IBM 7090.

The levels chosen were 1000, 925, 850, 775, 700, 600, 500, 400, 300, 250, 200, 150 and 100 mb. Besides height and wind the input data also included temperature for a more correct height interpolation and for a hydrostatic check. Rejected soundings were later on corrected and, together with those for which extrapolation to 1000 mb was required, they were used only for a separate computation of additional coefficients in the horizontal fields. These computations were made using the equation

$$\frac{1}{P}\int_P zF_k\,dp = z_k,$$

where for each F_k a mean value was taken for the October period.

The processing of wind data included separation into components and linear interpolation in order to obtain values for levels not given in the reports. The assumption of a linear wind profile, which was made in order to simplify the program, is of course very crude at levels where the pressure functions show large curvature. These points have therefore not been used in the analysis of the results. The pressure interval in the wind computations started at 925 mb. Since data for this level are not usually

24-hour height changes. The pressure interval was 300–1000 mb. The convergence in the expansion was found to be so rapid, that a reasonable accuracy could be obtained using only two modes. A continuation of this work has, however, not yet been reported.

TABLE 1.

	Date						
	21.10	22.10	23.10	24.10	25.10	26.10	27.10
No. of soundings used for computation of F_k and Z_k	327	281	292	275	286	330	286
No. of soundings rejected by hydrostatic check	40	48	31	29	34	18	30
No. of soundings corrected or extrapolated to 1000 mb	78	70	44	65	57	41	50
No. of wind observations	220	183	187	176	161	185	180

given in the reports, the 950 mb winds were simply taken without correction. In about 10 per cent of the cases where 950 mb winds were missing, 850 mb winds were used, again without correction.

Table 1 gives the number of observations that have been used in the computations for each separate day of the October period.

4. Results from expansion of height

Very little day to day variation was found in the general form of the functions $F_k(p)$ and it is therefore sufficient to show, Fig. 2, the results from one of the days. The curves have been drawn to go as smoothly as possible through all points computed. It is obvious from Fig. 2 that surface and stratospheric variations are taken up only to a reduced extent by the first mode,

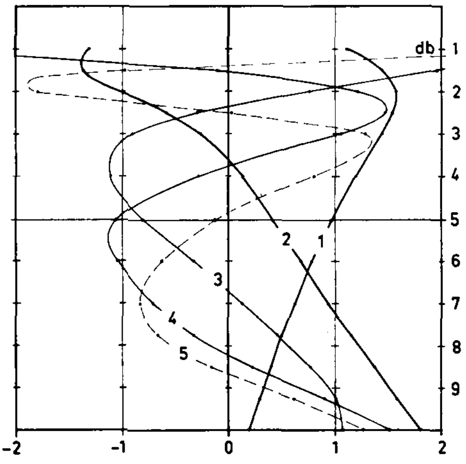

FIG. 2. Pressure functions $F_k(p)$ in expansion of height data for 24.10.1959. The figures indicate mode number.

which instead is dominated by conditions in the middle and upper troposphere with a maximum between 200 and 250 mb. The second mode in the interval considered has its highest value at 1000 mb and will therefore be dominated by height variations in the lower troposphere. These will also to some extent be taken up in the higher modes, but one should note that the influence from stratospheric height variations will gradually increase with the mode number.

The convergence of the series is surprisingly rapid. The r.m.s. values of the first five coefficients (in meters) are given in Table 2 for 18.6 and for the days in the October period. These values show the dominant character of the first mode and they also indicate from the values of the corresponding F-functions that the fourth and the fifth modes represent height variations that at almost all levels are comparable with observational errors.

This is also evident from the r.m.s. values of the residuals (in meters), the vertical distributions of which are shown for one of the days in Fig. 3. The thick curve to the right represents total variation of height (r.m.s. of Z) while the other curves give r.m.s. values of the residuals for an increased number of terms in the expansion. It is seen that most of the height variation in the troposphere is taken up by the first mode. With the second mode present the residuals are further decreased except in the vicinity of 400 mb, where the curves are in contact (since $F_2(p)$ vanishes at that level). With the third mode present the residuals are reduced to below 20 m in the interval 125–1000 mb. With regard to the normal accuracy in initial data one would expect the observational errors to have a rather big influence on the form of the higher modes. Since these show no irregularities and in their

TABLE 2.

Mode no.	Date							
	18.6	21.10	22.10	23.10	24.10	25.10	26.10	27.10
1	139	231	234	243	242	229	242	232
2	37	44	43	44	40	38	43	45
3	21	18	22	20	22	19	18	21
4	11	11	10	10	9	10	11	10
5	—	6	6	6	5	6	7	7

general form seem to be consistent with the lower mode curves, one may assume that the errors mostly are even more unsystematic and therefore taken up in still higher modes. On the other hand, it is obvious that even if the fourth and the fifth modes represent real atmospheric conditions, their part in the total variance is so small that for most purposes they can be completely neglected. In order to demonstrate this point even more clearly, r.m.s. values for the residuals are shown in Fig. 4 in terms of per cent of the total variation.

Since similar results are also obtained for all the other cases that so far have been investigated, it is evident that three parameters are sufficient and for many purposes even more than sufficient for a description of the height field.

For practical application, however, it is also necessary that the pressure functions are conservative. In this respect the results from the October period indicate that the lowest modes do not change from day to day but also that there is a tendency for increasing day to day variability with higher mode number. Taking time averages over the October period of the functions F_k we calculate the standard deviations at different levels (Fig. 5). It is seen that a main part of the interdiurnal variation is concentrated in the top and the bottom of the atmosphere. The total standard deviations, including all levels, are 0.016, 0.086 and 0.133 for the first three modes.

During this period large changes in the flow pattern occurred due to travelling waves and to some pronounced baroclinic developments. One may therefore assume that the uneven distribution of the observation stations and the variation in data coverage (see Table 1) are responsible for a significant part of the standard deviations given above and that even smaller values would be obtained with a more elaborate

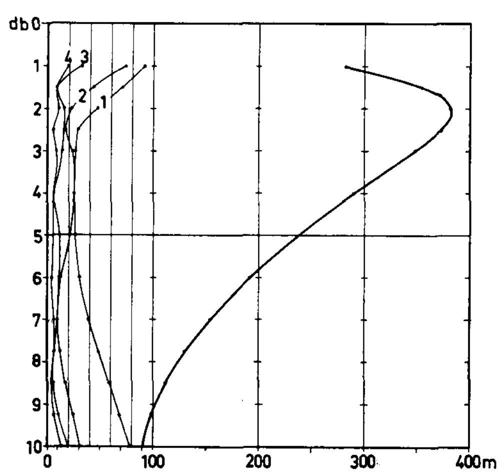

FIG. 3. Vertical distribution of residuals in expansion of height for 24.10.1959.

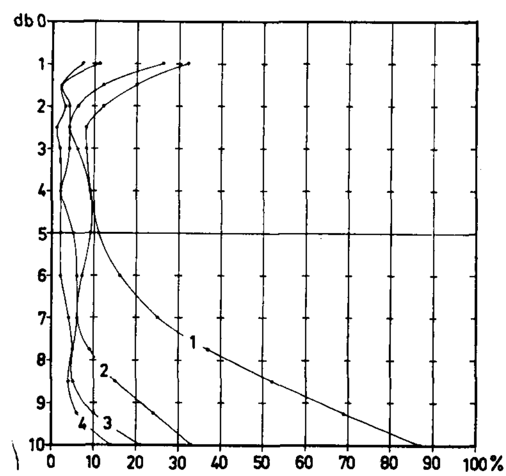

FIG. 4. Vertical distribution of residuals in per cent of the total r.m.s. variation at each level.

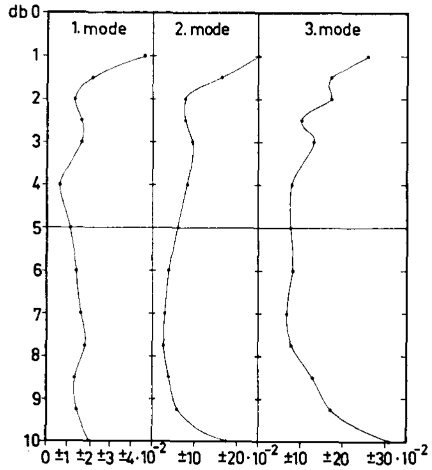

FIG. 5. Interdiurnal variation of $F_1(p)$, $F_2(p)$, and $F_3(p)$ expressed as standard deviation from mean of the October period.

choice of basic data. Therefore it seems clear that the first three modes may very well be conservative over periods that are long in comparison with those covered by ordinary numerical forecasts.

Some information regarding the seasonal variation in the mode form is found in Figs. 6*a*, *b* and *c*. Here mean modes for the October period are compared with corresponding modes for 18.6.1959 and also with modes calculated in one of the first tests, where data were randomly selected from the months December 1958 and January 1959 (altogether about 100 soundings

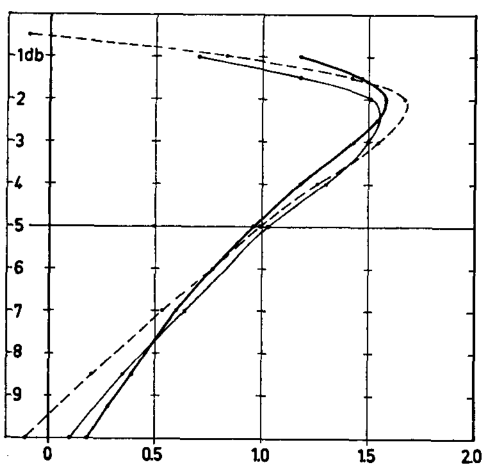

Fig. 6*a*.

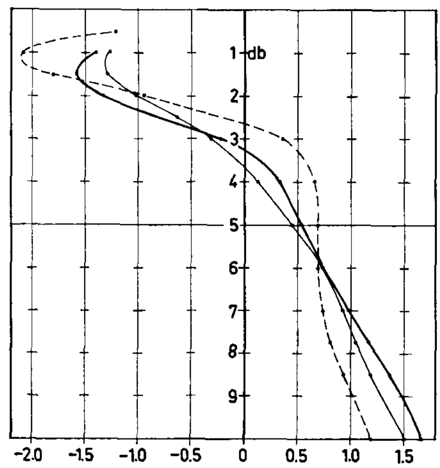

Fig. 6*b*.

extending to 50 mb). It is seen that the general form of the modes is preserved, but again rather large differences in data coverage make a detailed comparison difficult. The question needs further investigation.

In practical application of the expansion in natural orthogonal functions one will primarily be interested in the horizontal fields of the coefficients which for practical purposes will have to be determined with the aid of some adopted standard form of the pressure functions

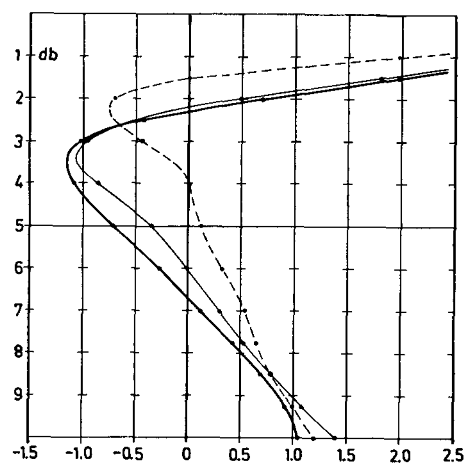

Fig. 6*c*.

FIG. 6. Examples indicating seasonal variation in (*a*) $F_1(p)$, (*b*) $F_2(p)$, and (*c*) $F_3(p)$. The thick full lines represent averages for the October period, thin full lines 18.6.1959 and thin broken lines results from a test computation (see text).

TABLE 3.

Case	Coefficient	R.m.s. variation due to mode no. 1	2	3	Total r.m.s. variation	Relative variation in per cent
1	z_1	0.1	0.9	0.1	0.9	0.3
	z_2	4.9	0.3	1.5	5.1	11.8
	z_3	1.0	3.3	0.2	3.4	16.5
2	z_1	1.7	1.7	2.3	3.3	1.4
	z_2	9.4	0.7	2.9	9.9	23.0
	z_3	22.3	5.6	0.5	23.0	109.5

(monthly mean values or equivalent). It is therefore of some interest to see the influence that a variation in the pressure functions will have on the computed values of the coefficients. Let us consider two different expansions

$$z = \sum z_k F_k = \sum z'_k F'_k.$$

Multiplying here by F'_n and taking a vertical average, we obtain

$$z'_n = \frac{1}{P} \sum_k z_k \int_P F_k F'_n \, dp.$$

Now let $F'_n = F_n + \Delta F_n$. Noting, furthermore, that both sets of pressure functions must be normalized, we find

$$z'_n = z_n \left(1 - \frac{1}{2P} \int_P \Delta F_n^2 \, dp\right) + \frac{1}{P} \sum_{k \neq n} z_k \int_P F_k \Delta F_n \, dp.$$

Values for $z_n - z'_n$ have been evaluated for two different cases, taking n and k equal to 1, 2 and 3. In the first case, where ΔF_n is chosen to be small, F_n represents a mean for the October period and F'_n one of these days (26.10). In the second F_n is unchanged but for F'_n values are taken from 18.6.1959. This choice will make ΔF_n larger than in a case where monthly mean values are used. The result is given in Table 3. The values chosen for z_1, z_2 and z_3 are in both cases 242, 43 and 21 respectively.

The result here depends naturally on the correlation between the pressure functions and their variations. The distribution of the latter has in these examples been chosen in an arbitrary way. It seems, however, that one can conclude that the field in the first mode is quite insensitive to comparatively large variations in the pressure functions and that this is true to some extent also for the second mode. With regard to the third mode the situation is different and the field is defined only if the proper pressure function is known.

Regarding, finally, the averaged pressure function $F_0(p)$, one can expect, in addition to a seasonal change, short period fluctuations due to variations in non-adiabatic heating and cooling and to differences in release of kinetic energy. A correct determination of the variation in the area average is difficult to make from available data since again differences in the data coverage will influence the result. During the October period the averaged height values show first an increase at all levels and then a steady decrease, again at all levels. A computation of the standard deviations from the mean gives 48 m at 250 mb and 10 m at 1000 mb and the r.m.s. value, integrated over all levels, is 30.5 m.

Whether a variability of this magnitude is serious or not depends on the specific purpose for the expansion in empirical orthogonal functions. For numerical weather prediction a general lifting or lowering of all pressure levels is not important since we are here primarily interested in gradients of the fields. It should be pointed out, however, that the deviations are not randomly distributed but have instead a vertical profile that is well described by the form of the function $F_1(p)$. Thus, writing

$$F_0(p,t) = F_{00}(p) + h_1(t) F_1(p) + r(p,t),$$

where F_{00} represents the time average for the October period, we find the values for h_1 in meters given in the following table

	Date						
	21.10	22.10	23.10	24.10	25.10	26.10	27.10
h_1	7.1	35.5	18.3	22.6	2.2	−34.3	−50.3

The r.m.s. value of the residual is reduced from 30.5 to 5.5 m. From this limited material it seems that short period fluctuations in the average atmosphere may be expressed through a general increase or decrease in the first mode coefficients. Comparing the October period with 18.6.1959 also indicates that the main part of the seasonal variation in F_0 can be taken care of in the same way but the second mode must also be included in order to reduce the residual below 10 m. However, further investigation is required before definite conclusions can be drawn and general methods developed.

In concluding this section a few words should be said about the alternative possibility to expand 24- or 12-hour height changes. This has been suggested during some discussions and was actually done by Obukhov (loc. cit.). As was shown by him, the first mode in this case is also dominant. The reason is clearly that the coefficients in the second and all higher modes are and remain so small that even if these fields were completely changed through advection over the area, their contribution to the total height changes at 500 mb, for instance, would be only a very small part of what is actually observed.

5. The thermal field

More interesting than the average height F_0 is the corresponding distribution of the static stability, σ, and its variations. The static stability is here defined as

$$\sigma = g\left(\frac{\partial^2 Z}{\partial p^2} + \frac{\varkappa}{p}\frac{\partial Z}{\partial p}\right), \tag{5.1}$$

where $\varkappa = Cv/Cp$.

Defining
$$\sigma_k = g\left(\frac{\partial^2 F_k}{\partial p^2} + \frac{\varkappa}{p}\frac{\partial F_k}{\partial p}\right), \tag{5.2}$$

we have the expansion

$$\sigma = \sigma_0 + \sum z_k \sigma_k. \tag{5.3}$$

TABLE 4.

p, mb	σ_0, m^2 sec^{-2} cb^{-2}	σ_1 ($\times 10^{-2}$) m sec^{-2} cb^{-2}
150	83.7	−5.65
200	41.3	−5.27
250	20.7	−3.46
300	8.9	−1.25
350	6.1	−0.43
400	4.4	−0.18
450	3.6	−0.02
500	3.0	0.05
550	2.8	0.06
600	2.5	0.05
650	2.2	0.04
700	2.2	0.02
750	2.1	0.00
800	1.9	−0.02
850	1.8	−0.06
900	2.1	−0.16
925	2.4	−0.23

Values for σ_0 and σ_1, computed from time averages of F_0 and F_1 over the October period, are given in Table 4.

The interpolation and smoothing have been carried out on the corresponding temperature profiles for which a regular behaviour has been assumed. This procedure is supposed to give correct values for σ_0, and the values found are similar to those given by GATES (1961*b*) for January, based on data from 45 U.S. radiosonde stations. In σ_1 the accuracy is low in the last decimal, but taking the order of magnitude to be correct, it is seen that the short period fluctuations in F_0 discussed at the end of the previous section will have almost no influence on the average static stability. With an r.m.s. value for z_1 of 250 m in the first mode of the height field, it is also seen that local variations in the static stability will in general be small in the pressure interval 400–850 mb. Below 850 mb and around the tropopause the variations will become significant, especially in deep lows, where z_1 may have values down to −600 m.

This result is also obvious from the series that can be obtained for the temperature by differentiating the expansion of Z with respect to p and making use of the hydrostatic relation. This gives

$$T = -\frac{gp}{R}\frac{\partial Z}{\partial p} = -\frac{gp}{R}\left(\frac{dF_0}{dp} + \sum z_k \frac{dF_k}{dp}\right).$$

For the purpose of similarity we write this relation in the form

$$T = T_0(p) + \sum T_k(x_1 y)\, \tau_k(p), \tag{5.4}$$

where

$$\tau_k(p) = -\frac{1}{\left[\frac{1}{P}\int_P \left(p\frac{dF_k}{dp}\right)^2 dp\right]^{\frac{1}{2}}} p \frac{dF_k}{dp} \tag{5.5}$$

and
$$T_k = \frac{g z_k}{R}\left[\frac{1}{P}\int_P \left(p\frac{dF_k}{dp}\right)^2 dp\right]^{\frac{1}{2}}. \tag{5.6}$$

The pressure functions $\tau_k(p)$ are here normalized in the same way as $F_k(p)$. In $F_k(p)$ the variation with p will be more rapid in higher modes than in the lower ones. The value of the normalizing factor, seen in the denominator of (5.5), will therefore increase with the mode number. It follows then from (5.6) that the convergence in the temperature expansion will be less rapid than the convergence in the expansion of height. It is furthermore clear that the expansion will not be efficient with regard to such pronounced details of the temperature profiles as subsidence or frontal inversions, which are of interest in the synoptic analysis. Since these inversions may occur at practically any height in the troposphere, they cannot be reflected directly in the form obtained for one single pressure function. An abrupt change in the vertical temperature gradient will therefore require a large number of modes for accurate representation.

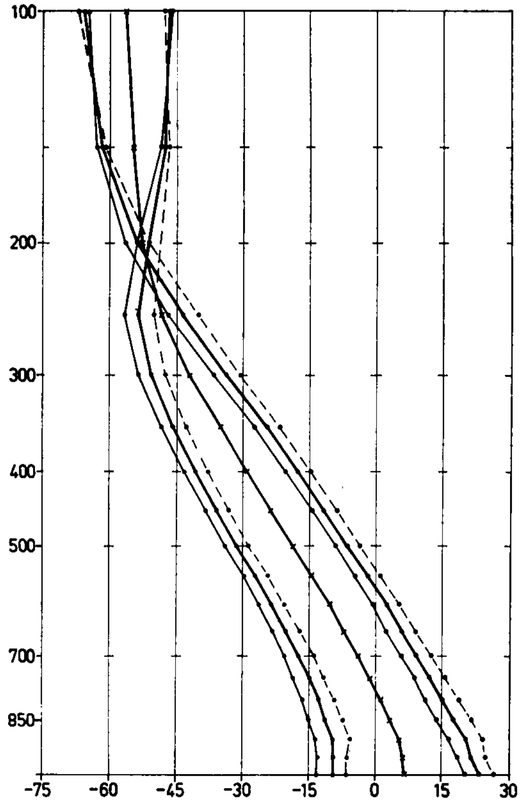

FIG. 8. Examples of temperature profiles, taking the standard atmosphere and first and second mode successively into account.

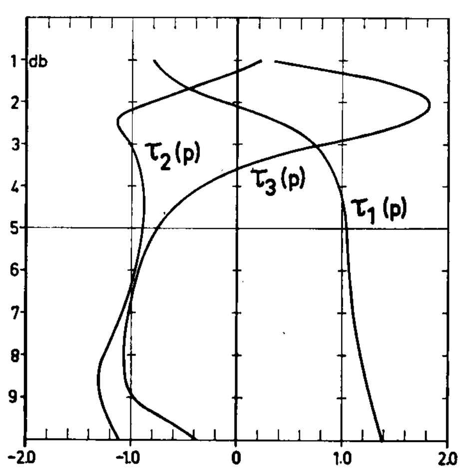

FIG. 7. Pressure functions for temperature derived from corresponding mean pressure functions for height.

On the other hand, it is interesting to notice that some general features in the thermal field which are important for the large scale dynamics are fairly well represented already in the first mode or in the first and the second modes. In Fig. 7 the first three functions $\tau_k(p)$ derived from $F_k(p)$ for 24.10 are shown. It is seen that $\tau_1(p)$ and $\tau_2(p)$ are almost constant in the main part of the troposphere and therefore in this interval will increase or decrease the temperature but have very little influence on the vertical temperature gradient. The main contribution to variations in the temperature gradient is centered around the tropopause level. This is also obvious in Fig. 8, where examples of temperature curves have been drawn, corresponding to

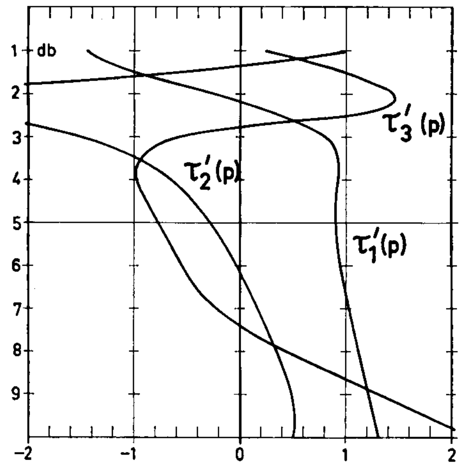

FIG. 9. Pressure functions for temperature expansion directly determined from temperature data.

$$T_0(p);\quad T_0(p) \pm 12\tau_1(p) \quad \text{and} \quad T_0(p) \pm \pm 12\tau_1(p) \pm 3\tau_2(p$$

Here the coefficient $T_1 = 12$ corresponds to $z_1 = 350$ m and $T_2 = 3$ to $z_2 = 55$ m. These values are slightly higher than the observed r.m.s. values. In Fig. 8 it is seen that even in the one-parameter representation one can describe not only a warm or cool troposphere but also variations in the height of the tropopause.

So far the parameters considered have been determined through height values. It is of course also possible to define the state of the atmosphere directly through the thermal field and expand the temperature in its own empirical orthogonal functions. In order to see if this would lead to an increase in the convergence, a test was made on data for 18.6.1959. The pressure functions from this expansion are shown in Fig. 9. Standard deviations from the horizontal mean temperature gave here a vertical average of 6.7°C. The r.m.s. values of the coefficients were 6.1, 2.3 and 2.2°C for the first three modes.

It is interesting to compare these values from the direct expansion of the temperature with those that are obtained if the series expansion defined in (5.4)–(5.6) is used for the same day and with the proper $F_k(p)$ functions. The temperature coefficients corresponding to r.m.s. values of z_1, z_2 and z_3 are 4.8, 2.1 and 2.0°C and the convergence is thus slower. The material on which this test is made is very limited but it indicates that in the choice of expansion one should decide beforehand if one wants the fastest possible convergence in the height data or in the temperature data. This question is of some importance in relation to the use of the expansion in numerical forecasting. If an expansion of height is used, one may with the aid of the geostrophic approximation use the orthogonality properties of the modes in order to eliminate terms in the vorticity equation. A similar procedure is not possible in the thermodynamic equation since the function $F_k(p)$ will here appear in differentiated form. If, on the other hand, temperature data are directly expanded, one can make use of the orthogonality in the adiabatic equation but not in the vorticity equation.

6. Expansion of wind data

The important use that one has made of the concept of geostrophic balance in synoptic weather analysis as well as in dynamic meteorology makes it natural to investigate separately the extent to which this approximation is valid in different modes. With regard to the dominance of the first mode one can here expect geostrophic conditions to prevail, but higher modes could be ageostrophic to a relatively high extent without disturbing too much the general geostrophic balance in the total wind field.

In order to test this point the expansions of the wind components have been made according to

$$u = \sum u_k A_k(p); \quad v = \sum v_k B_k(p), \tag{6.1}$$

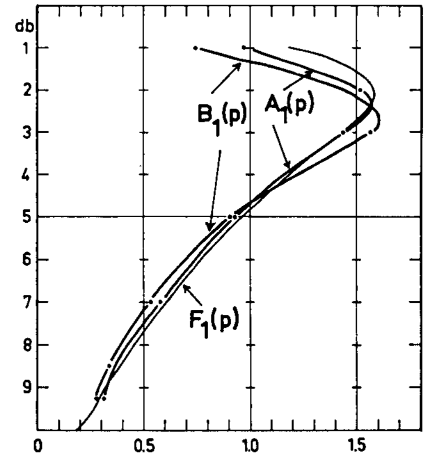

Fig. 10 *a*.

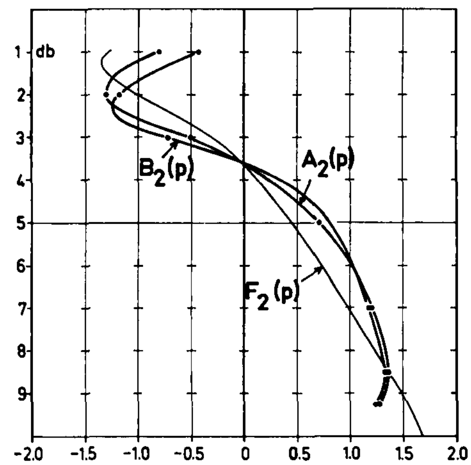

Fig. 10*b*.

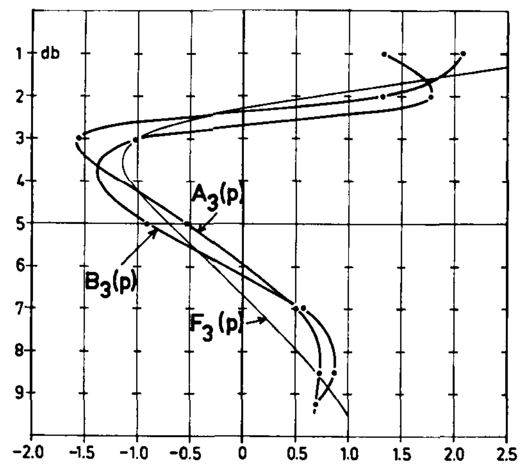

Fig. 10*c*.

FIG. 10. Pressure functions (*a*) A_1 and B_1, (*b*) A_2 and B_2 and (*c*) A_3 and B_3, from expansion of wind components.

with no term corresponding to $F_0(p)$. The pressure functions $A_k(p)$ and $B_k(p)$ have been normalized in the same way as $F_k(p)$. The results (Figs. 10*a*, *b* and *c*) show that A_k and B_k are mutually very similar, even though they have been computed in independent expansions. They are also similar to the corresponding F_k. This is especially the case in the first mode, where time averages of the pressure functions for the October period are also given.

Day to day variations are more pronounced in A and B than in F. The vertical distribution of the standard deviations shows very little dependence on pressure. Vertically integrated values of the standard deviations are for the October period given in Table 5, where, for convenience, the corresponding values for F are repeated.

The larger variability is to be expected here, since the wind field in general is irregular with large relative variations. The basic material for each day is also more restricted (Table 1) and

TABLE 5.

Pressure function	1st mode	2nd mode	3rd mode
A	0.05	0.14	0.24
B	0.14	0.17	0.41
F	0.02	0.09	0.13

differences in data coverage will therefore have an increased influence.

In Table 6 r.m.s. values for the coefficients (in msec^{-1}) in the first five modes are given for 18.6 and for the October period. It is seen that the convergence, as far as momentum is concerned, is not very rapid if compared with the expansion of height data. Assuming a geostrophic balance we shall see that the difference may be explained as due to a general decrease of the characteristic scale of the modal field with increasing mode number.

However, before values are given on the scales a few words should be said about the distribution of kinetic energy in different modes. A vertical integration shows that in the average during the October period 83 per cent of the total kinetic energy is represented by the first mode. The following four modes contain 7, 3, 1 and 1 per cent respectively. The remaining 5 per cent falls on still higher modes. A more detailed picture of the kinetic energy distribution is obtained with the aid of the residuals at different levels. These are shown in Fig. 11, where a measure of the kinetic energy has been computed simply by multiplying the r.m.s. values of the component coefficients by their proper pressure functions and then squaring and adding.

Regarding the seasonal variation of the kinetic energy a comparison between 18.6.1959

TABLE 6.

	Date															
	18.6		21.10		22.10		23.10		24.10		25.10		26.10		27.10	
Mode no.	u	v	u	v	u	v	u	v	u	v	u	v	u	v	u	v
1	10	7	13	8	14	8	13	8	15	10	15	11	16	9	14	8
2	4	3	4	3	4	4	4	3	4	3	3	3	3	3	4	3
3	3	2	3	2	2	2	3	2	2	2	2	2	2	2	2	2
4	2	2	2	1	2	1	2	1	2	2	2	1	2	1	1	1
5	—	—	1	1	1	1	1	1	1	1	1	1	1	1	1	1

and the October period reveals an interesting feature. For 18.6 the kinetic energy contained in each of the first four modes is 149, 25, 13 and 8 respectively, the measure being the same as above. In the average during the October period it is 285, 24, 9 and 5. It is seen that the energy level changes considerably in the first mode while in higher modes it remains relatively constant. The same tendency is also obvious in short period fluctuations, as can be seen from Table 6. One may therefore conclude that a major part of the kinetic energy produced in the atmosphere is fed into the first mode, either directly or through a non-linear interaction. Since low level winds in the first mode are comparatively weak it seems also reasonable to assume that the dissipation here is, relatively, less important than in the higher modes.

There is one point in the previous discussion that needs some further comments. In forming the measure of kinetic energy in each mode, we have squared and added r.m.s. values for the corresponding coefficients u_k and v_k. From the way in which these have been determined there is, however, no absolute reason why they should characterize the same specific property of the atmospheric field of motion. Taking an extreme case, it could, for instance, have happened that the second mode had been so dominant in the meridional motion that the iterative procedure in the computations had, independent of the first guess, converged towards v_2 and B_2 instead of v_1 and B_1.

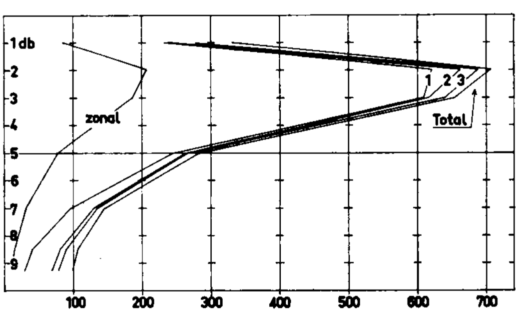

FIG. 11. Vertical distribution of kinetic energy in different modes. The curve to the left gives the kinetic energy in the mean zonal wind which entirely falls in the first mode.

Therefore in the foregoing we have tacitly used the hypothesis that corresponding modes in A, B and F (same mode number) are interrelated in a definite way and that they all reflect the same property in the vertical structure of the atmosphere. This working hypothesis, which seems to be necessary for the interpretation of the results, is based on the striking similarity between the functions and on the well-established existence of quasigeostrophic balance where non-linear terms are of little importance. A more general discussion of this and related problems will be given in a following paper and we shall therefore here use the hypothesis without any further comments.

Let us now return to the question of the scale in the coefficient fields. The similarity between the functions F, A and B makes it natural to write the condition for geostrophic balance as

$$f\mathbf{k} \times \sum \mathbf{v}_k F_k = -g \sum \nabla z_k F_k. \qquad (6.2)$$

We shall also, for convenience, introduce the following notations for the vertical and the horizontal averages of a quantity α.

$$\bar{\alpha} = \frac{1}{P}\int_P \alpha dp, \quad \tilde{\alpha} = \frac{1}{S}\int_S \alpha dS. \qquad (6.3)$$

Now multiplying (6.2) by F_n and taking a vertical average, we have, due to orthogonality and to normalization,

$$f\mathbf{k}\times\mathbf{v}_n = -g\nabla z_n.$$

Squaring both sides and denoting the absolute value of $\mathbf{v}_n$ by V_n, we find

$$\widetilde{f^2V_n^2} \simeq f_0^2\widetilde{V_n^2} = g^2[\widetilde{\nabla(z_n\nabla z_n)} - \widetilde{z_n\nabla^2 z_n}]$$

where f_0 is a mean value for the Coriolis parameter. Provided the area is sufficiently large, the first term on the right-hand side will tend to vanish. Introducing a generalized horizontal wave number k, such that

$$\nabla^2 z_n \simeq -k_n^2 z_n,$$

we obtain
$$k_n^2 = \frac{f_0^2\widetilde{V_n^2}}{g^2\widetilde{z_n^2}}. \tag{6.4}$$

In order to have a rough estimate of the scales, we can here use the r.m.s. values for z_n, u_n and v_n. The result in terms of wave-length, L in km, and hemispheric wave-number at 45° lat. n, is given in Table 7.

These figures represent only some kind of weighted mean over the spectral distributions for each mode. In the first mode the longitudinal spectrum extends to wave number zero corresponding to a zonal wind, for which the kinetic energy was given in Fig. 11. For the higher modes the zonal wind is non-existent. Between the first and the second modes the difference in the scale of the perturbation is therefore very small. For higher modes the values in Table 7 show that the spectra will be more and more dominated by small scale flow patterns.

7. Horizontal fields

The variation in scale with mode number is also clearly seen in the maps of the coefficient fields. It is the purpose here only to show a sample of such modal maps and to discuss some of their properties. In plotting the maps the values for the height coefficients have been directly entered. Data from extrapolated or otherwise corrected soundings have been underlined. Especially over mountainous regions these values seem not to be always correct and have therefore when necessary been left out of consideration in the analysis. The winds have been plotted in the usual way after the coefficients for the components have been combined into direction and velocity.

The isolines for the first mode map are shown in Fig. 12, for each 40 m. Since $F_1(p)\simeq 1$ at 500 mb, the line density will closely correspond to what is found on an ordinary 500 mb map. A comparison between Fig. 12 and Fig. 13, where the 500 mb map for the same observation time is shown, demonstrates immediately the very close similarity between the two fields. This was to be expected since the residuals, shown in Fig. 3, are small.

More conveniently it is also shown in Table 8, where as averages for the October period the contributions from different terms as well as the residuals in the expansion of height are given. For the pressure functions ordinary averages are taken, while for the coefficients and the residuals total r.m.s. values have been used. It is seen from the table that a somewhat closer similarity could have been obtained with a different line density in the first mode map and a comparison with the 400 mb field. Also the 300 mb field is obviously quite well represented by only one mode.

In general the ageostrophic wind components are smaller in the first mode map than at 500 mb. The modal map is also smoother and therefore easier to analyse. The reason is that irregularities and observational errors, which mostly have a random vertical distribution, cannot affect the first mode coefficients due to

TABLE 7.

	Mode no.							
	1		2		3		4	
	L	n	L	n	L	n	L	n
Mean 21–27.10	8900	3.2	5500	5.2	4000	7.0	2800	10.1
18.6	7100	4.0	5100	5.6	4000	7.0	2400	11.6

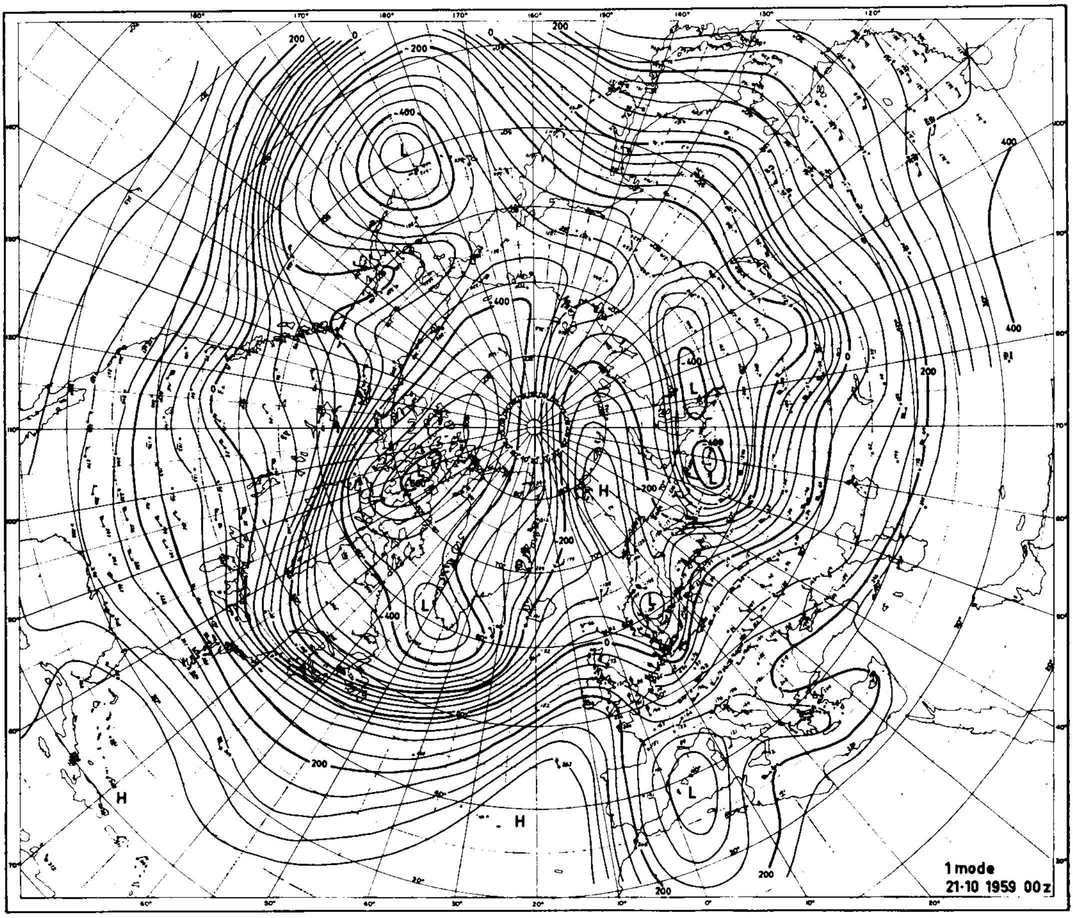

FIG. 12. First mode field of height coefficients and winds for 21.10.1959 OOZ. Isolines are drawn for each 40 m in z_1.

TABLE 8.

p	F_0	z_1F_1	r_1	z_2F_2	r_2	z_3F_3	r_3
100	16,175	278	90	53	71	62	35
150	13,624	347	68	54	41	40	9
200	11,790	373	49	43	22	14	18
250	10,348	363	32	26	18	8	15
300	9,145	337	28	13	24	20	13
400	7,165	278	24	5	23	22	7
500	5,550	227	26	19	18	14	11
600	4,178	182	34	31	13	5	12
700	2,984	142	43	41	10	2	10
775	2,179	116	51	50	11	8	7
850	1,440	90	60	58	15	14	6
925	754	66	69	65	22	19	12
1000	119	42	79	70	34	21	25

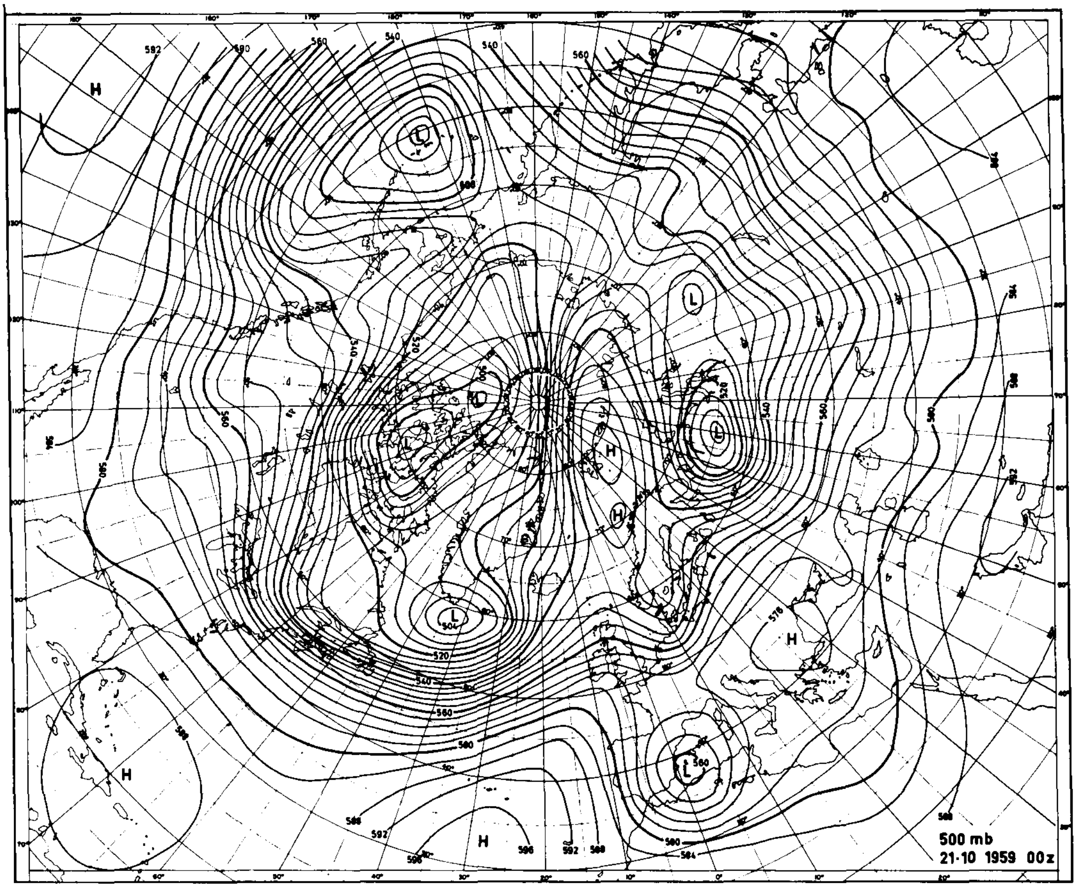

FIG. 13. The 500-mb map for 21.10.1959 OOZ.

the vertical integration. They will be taken up by higher modes.

In the second mode map, Fig. 14, the isolines have been drawn for each 20 m since the gradients are much weaker. Also here the winds show, with regard to direction, a pronounced tendency for geostrophic balance. Contrary to the first mode field, the second mode shows no systematic meridional distribution of the height coefficients and therefore the zero hemispheric wave number is not present in the flow pattern. Instead wave-numbers 1, 2 and 3 seem to be well represented. They show throughout the period a stationary character. During the seven days investigated the Sibirian high and the lows over the northern Pacific and over the Mexican Gulf do not move. The high over the U.S.A. is slowly weakening and towards the end of the period it is replaced by a low, which is formed over the area. At the same time the high, which on 21.10 is found south of 40° N over the Atlantic, builds up and extends towards 60° N. We find here the very small or even vanishing phase velocities that are typical for ultra long waves. Since waves of this type are also present in the first mode one may expect that interaction between the first two modes would play some role in determining the phase speed.

It is seen in Table 8 that a relatively large contribution to the height field is given by the second mode only in the lowest parts of the troposphere. It is therefore to be expected that the second mode should show some characteristic features of the surface map. This is also clearly seen in Fig. 14, where surface fronts

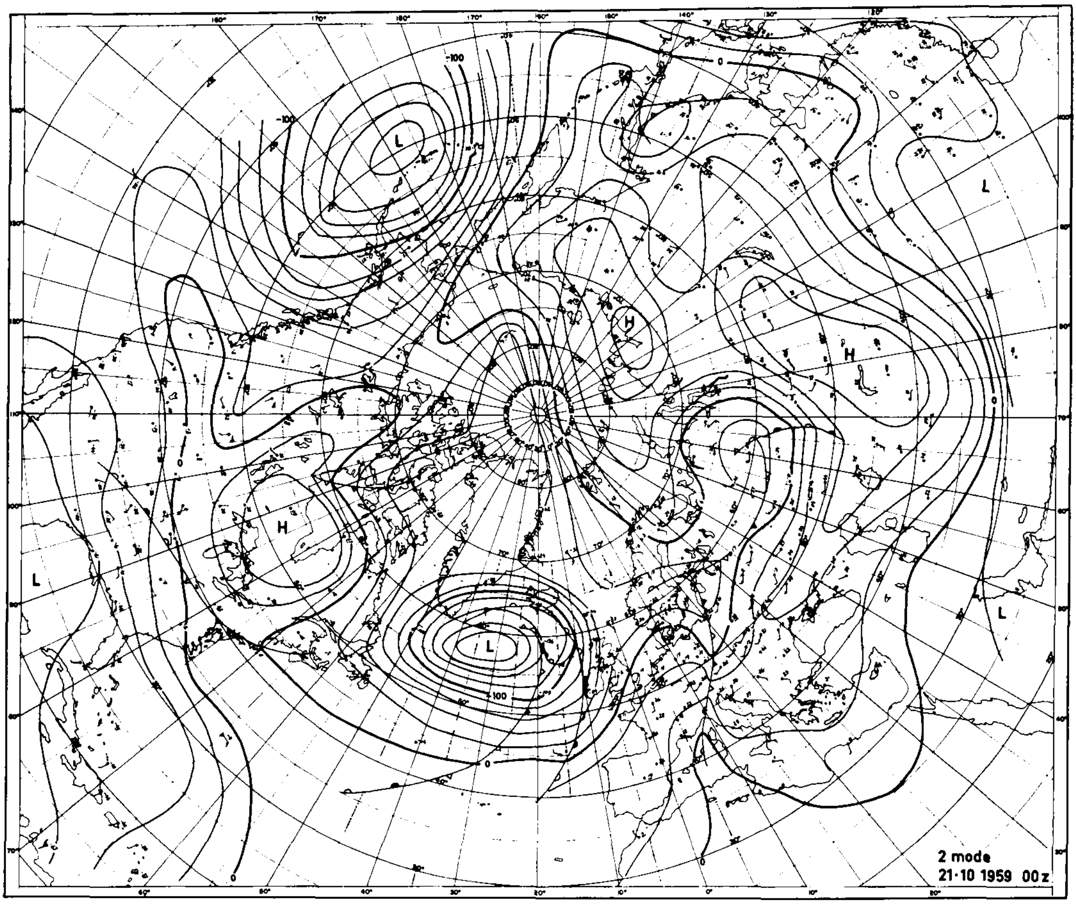

FIG. 14. Second mode field of height coefficients and winds for 21.10.1959 OOZ. Isolines are drawn for each 20 m in z_2.

have been drawn in the positions given on the ordinary Weather Service analysis. Analysis of the remaining maps in the period shows that active fronts can without difficulty be identified with pronounced small scale troughs in the coefficient field.

The motion of these troughs as well as of other small scale disturbances is in general quite rapid and seems to be determined by advection in the first mode wind field. Thus the troughs over northern Europe move rapidly to the east, the center of the low south of Iceland and Greenland moves north and the trough over Canada towards southeast. We find illustrated here in a clearer way the steering mechanism which has been used in routine forecasting for relating the motion at the surface to the 500 mb flow.

In the third mode map, Fig. 15, the isolines have been drawn for each 10 m. The gradients are so weak that, using the same line density as in the first mode, one would mostly find only a zero line. Even if the field seems quite erratic, surprisingly little smoothing is required in the analysis and few data have been completely discarded. It is obvious from Table 8 that the third mode map will not be similar to any ordinary pressure level map. The motion of the configurations is in some cases quite rapid and seems then to be determined by advection in the first mode field. It is, however, difficult to follow the displacements over several days since the pattern is continuously being transformed with lows and highs dissolving or forming.

A few words should finally be added with

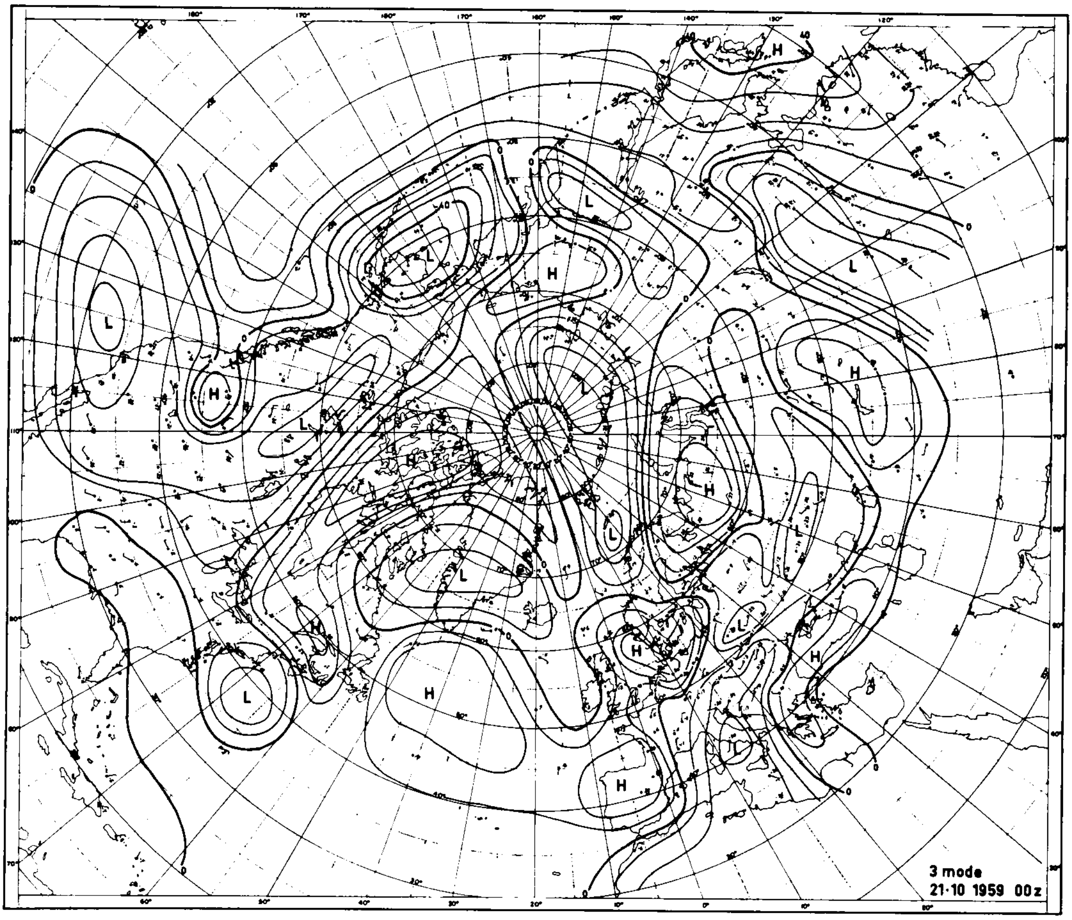

FIG. 15. Third mode field of height coefficients and winds for 21.10.1959 OOZ. Isolines are drawn for each 10 m in z_3.

regard to the correspondence between the first two modal fields. Due to the method for the expansion, the fields are uncorrelated and are therefore on an average out of phase when the same wave numbers are considered. This is, however, not necessarily the case at all places and pronounced deepenings in the total field at, for instance, a pressure level in the lower troposphere can therefore occur either as a result of a deepening in one or the other of the modal fields or from conservative lows in both fields becoming superimposed. The latter alternative seems to be contributing to many of the "baroclinic" developments that have occurred during the October period.

An example where this mechanism plays an important role is presented in Figs. 16*a*, *b*, and *c*, which show the development of the first and second mode fields during a period of two days. Second mode coefficient contours for each 20 m are drawn as full lines, while the thick broken lines represent 200 m contours for the first mode coefficients. Plotted observations relate to the second mode.

Comparing the maps one can directly see how the pattern in the second mode field is advected in the first mode wind field. By introducing the expansion in the vorticity equation it is easily shown that the advection will take place with a speed which is about 0.6 of

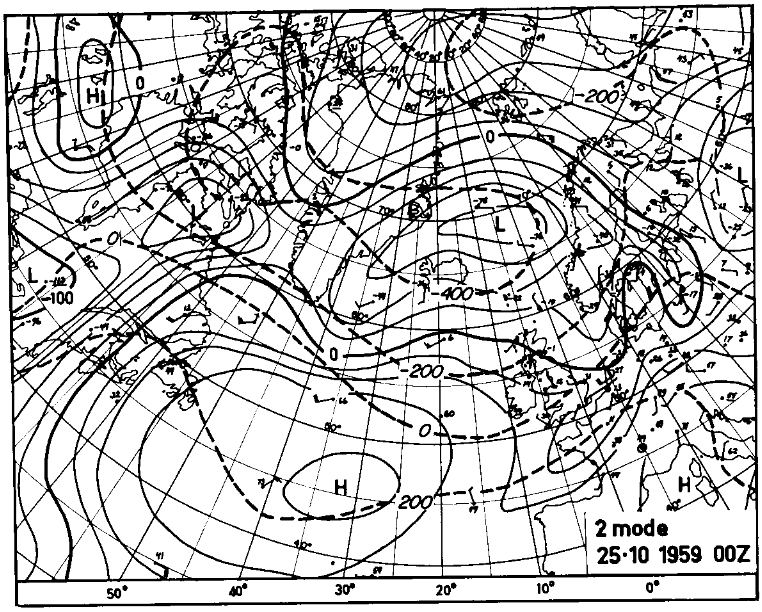

FIG. 16a. The situation on 25.10.1959 OOZ. Isolines for the second mode are drawn in full lines for each 20 m. The thick broken lines give the first mode coefficient field for each 200 m.

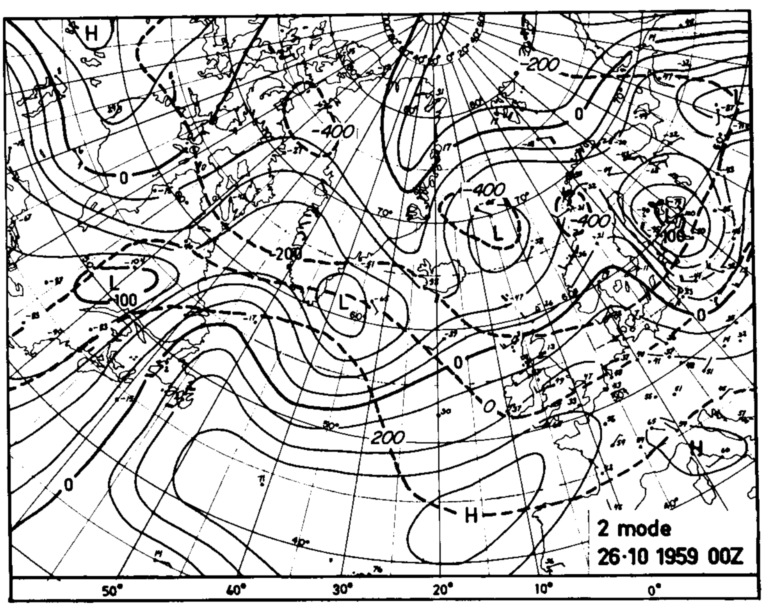

FIG. 16b. The situation on 26.10.1959 OOZ.

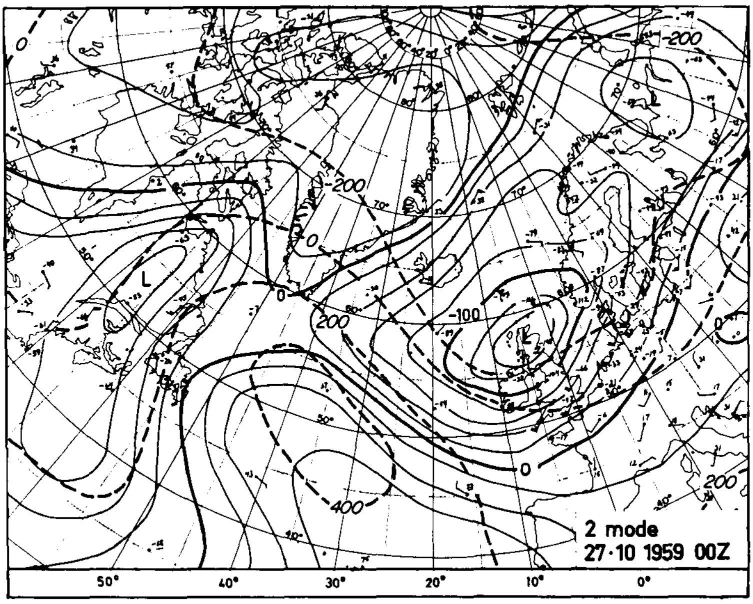

FIG. 16c. The situation on 27.10.1959 OOZ.

the first mode wind. This agrees well with the displacements that are observed during the period considered.[1]

Of particular interest is the movement of the second mode low, which on the 25th is observed over north-eastern Canada. It is situated in a strong westerly current in the first mode field and from the 25th to the 26th it is advected to a position east of southern Greenland. It is here superimposed on a ridge in the first mode field, while, further to the east, a ridge in the second mode over western Europe is superimposed on a trough in the first mode field.

The two fields are practically out of phase and therefore the resulting 500 and 700 mb fields do not show very pronounced perturbations in the westerlies. Due to advection the phase speed is in the second mode very much higher than in the first mode and already on October 27 the fields are in phase, resulting in a rather drastic change in the total circulation at 500 and 700 mb. It should also be observed that the second mode low has intensified during the advection towards southeast. The combined effect of advection and intensification results over the British Isles in a surface pressure fall of not less than 45 mb in 24 hours.

[1] It may be pointed out that some of the displacements observed in the first mode field may equally well be interpreted as due to advection in the second mode low level wind field.

8. Conclusion

In this attempt to determine suitable parameters for use in numerical forecasting the condition finally adopted was one of maximum descriptive capacity. Since this is a very general condition it is natural that the results should have a variety of possible practical applications. Through the discussion in the previous section of the coefficient fields it seems quite probable that these may provide useful tools in routine synoptic forecasting, primarily because the method admits a separation of the required information into a few uncorrelated but interacting fields.

It is not the purpose here to go into a detailed discussion of various aspects of the practical applications, but it should perhaps be noticed that the method, if experience shows that it can be used alone at a weather service, will give a definite reduction in the labour on a qualified level. Naturally the gain will be counterbalanced by the fact that the computation of modal coefficients from standard transmitted data will

TABLE 9.

Case	Field	Average contribution (in m) from mode no. 1	2	3	4	5
I	z^*	244	10	1	4	2
	z_m	226	19	14	9	0
	z'	119	37	7	9	2
II	z^*	207	25	2	8	4
	z_m	181	31	5	11	4
	z'	131	38	13	1	3

take considerable time at such weather services where automatic data processing does not yet exist or where processed data cannot be made available. There is no difficulty in constructing suitable diagrams for such computations, but the obvious solution would here rather be to have the computations made already at the observation stations as part of the regular program. Among other advantages this would make it possible to condense the information of immediate interest for routine services into a very short message.

Turning now to the problem of numerical forecasting, it may in the first instance be of interest to use the results obtained here in order to test the efficiency of conventional models. We shall here only consider two cases of two-parameter, finite difference models, the pressure levels taken to be 250, 500 and 750 mb in case I, 300, 600 and 900 mb in case II.

In Table 9 the average contributions are given for the October period from the first five modes to the r.m.s. variation in the mean field z^*, the middle field z_m and the difference field z'. It is seen that the mean fields as well as the middle fields are dominated by the contribution from the first mode and may therefore with a very good approximation be taken as representative for the first mode fields. Maximum efficiency is then obtained if the second parameter defines the second mode only or a combination of the second and higher modes. It is seen from Table 9, however, that the difference field on an average is also dominated by a contribution from the first mode. The prognostic equation for the difference field will therefore mainly be operating on information that is already taken care of by the prognostic equation for the mean field. This procedure is not only inefficient. There is also the probability that, due to inevitable model approximations, the covariant parts will not be handled in the same way by these two equations and will produce errors which, due to the dominance of the first mode, may be so large that they overshadow the small but important information initially given on the second and higher modes.

A corresponding result and eventually a better measure of the efficiency of the representation in a model is obtained if we determine the correlation coefficient between the variations in the mean field and in the difference field. It is in case I 0.85 and in case II 0.91. These figures, which have been computed for the October period and on the basis of the first five modes, are indeed very high, especially if compared with the vanishing correlation coefficients between the modal fields. They undoubtedly give the correct impression that the two-parameter models defined above will have very little possibility to be better than a conventional barotropic model if verification is made over a sufficiently large area. It should also be remembered, however, that the data given in Table 9 as well as the values of the correlation coefficients represent averages over the total area and over 7 days. Over limited areas the second mode may, especially if gradients are considered, carry a much larger weight in the difference field and the two-parameter model may therefore in such cases still show some superiority.

Considering, finally, the very natural approach to use the expansion directly in the thermohydrodynamic systems of equations, one will here meet a number of problems that will have to be solved before proper prognostic equations can be determined for the most important modes. It will be necessary to find corresponding expansions for the stream function and for the velocity potential, since these are not immediately given from observed data. One may in the first mode use the geostrophic approximation to relate the pressure function for the height to that of the stream function, but it is not immediately obvious that the same approximation holds sufficiently well when higher modes are considered.

For the first mode, where the pressure functions in general are small in the vicinity of 1000 mb, it seems probable that one should in a first approximation be able to neglect boundary effects. For the higher modes, however, the high values of the pressure functions close to the lower boundary make it probable that friction, topography or non-adiabatic heating cannot be neglected. In such a case these effects must, however, be introduced in a way that is sufficiently consistent with the empirical knowledge of the form of the pressure functions that will have to be used in constructing the model.

For these and other reasons it seems that one should in the first instance try to develop on a purely theoretical basis a dynamical system, where the modal properties of the atmosphere can be studied and compared with the empirical data. An attempt in this direction will be made in the following paper.

Acknowledgements

The author is indebted to Professor Bert Bolin and Dr. George Veronis for valuable comments on the manuscript and to Mr. Paul Crutzen for coding and running the program used, for data from July 18, 1959. Special thanks are due to Mr. Bengt Söderberg of the Swedish Air Force, who in an excellent way took care of the programming and the computations for the October period. The assistance of Mrs. Kerstin Willborg and Mrs. Mariana Domines in drawing the figures and carrying out numerous hand computations is also gratefully acknowledged.

REFERENCES

Bolin, B., 1953, Multiple-parameter models of the atmosphere for numerical forecasting purposes. *Tellus*, **5**, pp. 207–218.

Charney, J., 1949, On the physical basis for numerical prediction of large-scale motions in the atmosphere. *J. Meteor.*, **6**, pp. 371–385.

Gates, W. L., 1961*a*, The stability properties and energy transformations of the two-layer model of variable static stability. *Tellus*, **13**, pp. 460–470.

Gates, W. L., 1961*b*, Static stability measures in the atmosphere. *J. Meteor*, **18**, pp. 526–533.

Obukhov, A. M., 1960, The statistically orthogonal expansion of empirical functions. *Izvestiya Geophys. Ser.* 1960, pp. 288–291. (English translation from Известія, Серия Геофизическая, 1960, pp. 432–439.)